Alexandria Engineering Journal (2021) 60, 2641–2659

HOSTED BY ELSEVIER

Alexandria University

Alexandria Engineering Journal

www.elsevier.com/locate/aej
www.sciencedirect.com

A novel design of fractional Meyer wavelet neural networks with application to the nonlinear singular fractional Lane-Emden systems

Zulqurnain Sabir [a,*], **Muhammad Asif Zahoor Raja** [b,c], **Juan L.G. Guirao** [d,*], **Muhammad Shoaib** [e]

[a] *Department of Mathematics and Statistics, Hazara University, Mansehra, Pakistan*
[b] *Future Technology Research Center, National Yunlin University of Science and Technology, 123 University Road, Section 3, Douliou, Yunlin 64002, Taiwan, ROC*
[c] *Department of Electrical and Computer Engineering, COMSATS University Islamabad, Attock Campus, Attock 43600, Pakistan*
[d] *Department of Applied Mathematics and Statistics, Technical University of Cartagena, Hospital de Marina, 30203-Cartagena, Spain*
[e] *Department of Mathematics, COMSATS University Islamabad, Attock Campus, Attock 43600, Pakistan*

Received 16 November 2020; revised 20 December 2020; accepted 5 January 2021
Available online 18 January 2021

KEYWORDS

Meyer wavelet kernels;
Neural networks;
Hybrid computing techniques;
Lane-Emden equation;
Singular systems;
Stochastic computing

Abstract In this study, a novel stochastic computational frameworks based on fractional Meyer wavelet artificial neural network (FMW-ANN) is designed for nonlinear-singular fractional Lane-Emden (NS-FLE) differential equation. The modeling strength of FMW-ANN is used to transformed the differential NS-FLE system to difference equations and approximate theory is implemented in mean squared error sense to develop a merit function for NS-FLE differential equations. Meta-heuristic strength of hybrid computing by exploiting global search efficacy of genetic algorithms (GA) supported with local refinements with efficient active-set (AS) algorithm is used for optimization of design variables FMW-ANN., i.e., FMW-ANN-GASA. The proposed FMW-ANN-GASA methodology is implemented on NS-FLM for six different scenarios in order to exam the accuracy, convergence, stability and robustness. The proposed numerical results of FMW-ANN-GASA are compared with exact solutions to verify the correctness, viability and efficacy. The statistical observations further validate the worth of FMW-ANN-GASA for the solution of singular nonlinear fractional order systems.

1. Introduction

The study of fractional order differential equations (FDEs) is considered very important in almost all the field in-particular

* Corresponding authors.
E-mail addresses: zulqurnain_maths@hu.edu.pk (Z. Sabir), rajamaz@yuntect.edu.tw (M. Asif Zahoor Raja), juan.garcia@upct.es (J.L.G. Guirao), dr.shoaib@cuiatk.edu.pk (M. Shoaib).
Peer review under responsibility of Faculty of Engineering, Alexandria University.

https://doi.org/10.1016/j.aej.2021.01.004
1110-0168

mathematics, physics, control systems and engineering. Fractional calculus and FDEs have been studied during the last three decades using different operators: few of paramount significance are Erdlyi-Kober operator [1], operator of the Riemann-Liouville [2], Caputo operator [3], Weyl-Riesz operator [4] and Grnwald-Letnikov operator [5]. The study of these fractional derivative operators is extensive reported such as in the modeling of viscoplasticity [6–7], dynamic systems [8], thermal analysis of disk brakes [9], real materials [10], fluid mechanics [11], glass forming materials [12], electromagnetic theory [13], viscous dampers [14], fast desorption process of methane in coal [15], fractional tumor-immune model [16], generalize truncated M−fractional order derivative applications [17], fractional epidemiological model of computer virus propagation [18], fractional order SIR model for measles [19], fractional Harry Dym systems [20], deathly disease dynamics in pregnant women [21], time fractional wave equations [22], fractional Benney–Lin equation [23], Ablowitz-Kaup-Newell-Segur equation [24], fractional Fisher's type equations [25], fractal-fractional time delay equations [26], space–time fractional advection–diffusion equation [27], fractional neural networks for nonlinear system identification [28], fractional delay differential equations with variable order dynamics [29–30], a fractional model of chronic hepatitis C virus dynamics [31], deep brain stimulation systems [32], telegraph equation involving fractal derivatives [33], fractional Kdv–Burgers–Kuramoto systems [34], Fangzhu's nanoscale surface morphology [35], fractal nonlinear oscillator [36], fractal Burgers-BBM Equation [37] and many more [38–45].

There are many linear/nonlinear, singular/nonsingular, initial, boundary value problems (BVPs) are considered very complicated to solve with traditional procedure, one of such class is nonlinear singular Lane-Emden system that exists in astrophysics and normally consider to be very stiff to be solved due to existence of singularity at the origin. Many deterministic methods have been implemented to solve Lane-Emden models such as homotopy perturbation technique [46], sinc-collocation technique [47], variational iteration technique [48] and many more [49–52] etc. All these analytical/numerical schemes have their own individual merits and drawbacks over one another, while stochastic numerical solver based on soft computing or machine learning methodologies have not be yet exploiting to solve nonlinear-singular fractional Lane-Emden (NS-FLE) system. The normal form of NS-FLE equation is given as follows [53]:

$$D^{\alpha}y(x) + \frac{\lambda}{x^{\alpha-\beta}}D^{\beta}y(x) + f(x,y) = g(x), \tag{1}$$

$$y(0) = c_0, \quad y(1) = d_0$$

where $0 < x \leqslant 1,\ \lambda \geqslant 0,\ 0 < \alpha \leqslant 2,\ 0 < \beta \leqslant 1,\ c_0$ and d_0 are to be the constants, and D is fractional derivative operator. Aim of the present work is to determine the solution of (1) by exploiting the intelligent techniques on neural networks and their learning of parameters with hybrid *meta*-heuristic methodologies.

The *meta*-heuristic based numerical computing has been extensively implemented by the research community to solve solving nonlinear systems by functioning strength of neural networks (NN) and effective adaptation with evolutionary computing paradigms [54–58]. Recent reported studies are cell biology [59], nonlinear prey-predator models [60], nonlinear reactive transport model [61], nonlinear stiff differential system represented with Troesch's problem [62], nonlinear singular Thomas-Fermi systems [63], nonlinear doubly singular systems [64], micropolar fluid flow [65], magnetohydrodynamic flow [66], heartbeat model [67], control systems [68], nonlinear singular model arising heat distribution studies [69], power [70] and energy [71]. These contributions have proven worth and significance of stochastic numerical solvers on operators for convergence, accuracy and robustness.

Keeping in view all these application, stochastic technique are introduced for solving the NS-FLE equation as well. Aim of the presented work is to solve (1) by the design of intelligent computing through fractional Meyer wavelet artificial neural network (FM-ANN) optimized by the hybrid strength of genetic algorithm (GA) and active-set (AS), i.e., FMM-ANN-GAAS. The salient features of proposed FMM-ANN-GAAS are listed as follows:

- Novel design of fractional Meyer-wavelet neural network trained with integrated heuristics of GA aided with AS algorithm is presented for solving variants of fractional Lane-Emden system represented with singular nonlinear differential equations involving fractional derivative terms.
- The proposed FMM-ANN-GAAS scheme is applied for variants of NS-FLE systems and comparison of the results from available exact solution verify the correctness for solving these singular fractional order systems.
- The performance accreditation established through results of statistical investigation operators in terms of Theil's inequality coefficient, semi interquartile range, root mean square error and mean absolute error measures.
- The simple coherent structure of Meyer wavenets, availability of solutions on entire continuous training domain, smooth implementation procedure, reliable, robust, stability, extendibility are other worry assurances of the proposed stochastic numerical solver.

Remaining of the paper is organized as follows. In section 2, the design procedure adopted for formulation of Meyer wavenet and their optimizations with hybrid computation heuristics of GAAS algorithm. In Section 3, performance operators are presented. In Section 4, numerical outcomes of FM-ANN-GAAS are presented. In Section 5, the concluding remarks and future research opening are listed.

2. Designed methodology

The FMW-ANN is designed for solving singular FDEs in this section. The formulation for designing the differential equation models, fitness function, and optimization procedure based on combination of GA-ASA is presented here.

2.1. Fractional Meyer wavelet neural network

The ANN based models are exploited to provide the solution for different applications [72–73]. In the FMW-ANN; $\hat{y}(x)$is used for the proposed solution and its n^{th} order integer derivatives is $D^{(n)}\hat{y}(x)$ while the fractional order derivative is $D^{\alpha}\hat{y}(x)$, and expression of these networks are respectively given as:

$$\hat{y}(x) = \sum_{i=1}^{m} a_i f(b_i x + c_i) \tag{2}$$

$$D^{(n)}\hat{y}(x) = \sum_{i=1}^{m} a_i D^{(n)} f(b_i x + c_i)$$

$$D^{\alpha}\hat{y}(x) = \sum_{i=1}^{m} a_i D^{\alpha} f(b_i x + c_i)$$

where m represents the number of neurons, $\boldsymbol{a}$, $\boldsymbol{b}$ and $\boldsymbol{c}$ are the vector component of weight matrix $\boldsymbol{W}$ as:

$\boldsymbol{W} = [\boldsymbol{a}, \boldsymbol{b}, \boldsymbol{c}]$, for $\boldsymbol{a} = [a_1, a_2, ..., a_m]$, $\boldsymbol{b} = [b_1, b_2, ..., b_m]$ *and* $\boldsymbol{c} = [c_1, c_2, ..., c_m]$

while, the Meyer wavelet kernel is defined as:

$$f(x) = 35x^4 - 84x^5 + 70x^6 - 20x^7 \tag{3}$$

Using the Meyer wavelet kernel in the equation (3) in set of equations (2), we have:

$$\hat{y}(x) = \sum_{i=1}^{m} a_i \left(35(b_i x + c_i)^4 - 84(b_i x + c_i)^5 + 70(b_i x + c_i)^6 - 20(b_i x + c_i)^7\right), \tag{4}$$

$$D^{(n)}\hat{y}(x) = \sum_{i=1}^{m} a_i \begin{pmatrix} 35D^{(n)}(b_i x + c_i)^4 - 84D^{(n)}(b_i x + c_i)^5 + 70D^{(n)}(b_i x + c_i)^6 \\ -20D^{(n)}(b_i x + c_i)^7 \end{pmatrix},$$

$$D^{\alpha}\hat{y}(x) = \sum_{i=1}^{m} a_i \begin{pmatrix} 35D^{\alpha}(b_i x + c_i)^4 - 84D^{\alpha}(b_i x + c_i)^5 + 70D^{\alpha}(b_i x + c_i)^6 \\ -20D^{\alpha}(b_i x + c_i)^7 \end{pmatrix},$$

the arbitrary combination of the FMW-ANN can be used to solve NS-FLE system (1) subject to availability of appropriate weight matrix W. In order to determine the weights of FMW-ANN, one may exploit the approximation theory in mean squared error sense to formulate a fitness function E as:

$$E = E_1 + E_2 \tag{5}$$

where E_1 is the error function related to NS-FLE equation (1) and E_2 is used for initial conditions for the model (1), and are respectively given as:

$$E_1 = \frac{1}{N}\sum_{i=1}^{m}\left(D^{\alpha}\hat{y}_m + \frac{\lambda}{x_m^{\alpha-\beta}} D^{\beta}\hat{y}_m + f(x_m, y_m) - g_m\right)^2 \tag{6}$$

$$E_2 = \frac{1}{2}\left((\hat{y}_0 - A)^2 + (\hat{y}_N - B)^2\right) \tag{7}$$

for $N = \frac{1}{h}$, $\hat{y}_m = \hat{y}(x_m)$, $g_m = g(x_m)\, x_m = mh$.

One may determine the solution of NS-FLE (1) with the obtainability of suitable $\boldsymbol{W}$, such that fitness approach zero, the outcomes of FMW-ANN approximate the exact/optimal results, i.e., $[\hat{y} \to y]$.

2.2. Networks optimization

The optimization of parameter for FMW-ANN is carried out using the hybrid computing framework based on GAAS techniques.

Genetic Algorithm is an optimization solver for the constrained/unconstrained global optimization problems and formulated on mathematical modelling of natural genetic process. GAs continually changes a population of individual, i.e., candidate solutions of optimization task and has ability to solve a variety of optimization problems by incorporated its reproduction tools via crossover, selection, elitism and mutation operators. Recently applications address with GAs include optimization of steel space frames with semi-rigid connections [74], control structure for a car-like robot [75], modelling and identification of nonlinear multivariable systems [76], optimization of investments in Forex markets with high leverage [77], a fully customizable hardware implementation [78], characterization of hyperelastic materials [79], evaluation of apparent shear stress in prismatic compound channels [80], detection of loss of coolant accidents of nuclear power plants [81], torque estimation problem [82] and prediction of biosorption capacity [83]. GAs hybridized with local search technique can upgrade its laziness trough the optimization procedure.

Active-set algorithm is a viable local search methodology for rapid finetuning of optimization problem in different fields. Few renewed applications recently address effectively by AS algorithm are models of Sisko fluid flow and heat transfer [84], for optimization extreme learning machines [85], symmetric eigenvalue complementarity problem [86], induction motor models [87], sidescan sonar image segmentation [88] and cardiac defibrillation [89].

The integration of GAs with AS, i.e., GAAS, is exploited for finding the adjustables of FMW-ANN for solving the NS-FLE systems. The brief descriptive procedure of optimization with GAAS in pseudocode is presented in Table 1.

3. Performance indices

The performance measures, used to analyzing strength and weaknesses of proposed FMW-ANN-GASA methodology for solving the variants of NS-FLM system, incorporated in this study are Theil's inequality coefficient (TIC), mean absolute deviation (MAD) and root mean square error (RMSE) as well as their average gauges named as Global TIC (G-TIC), Global MAD (G-MAD), and Global RMSE (G-RMSE). The definitions of TIC, MAD and RMSE in terms of the exact solution y and approximate solution $\hat{y}$ are given, respectively, as:

$$\mathrm{TIC} = \frac{\sqrt{\frac{1}{n}\sum_{m=1}^{n}(y_m - \hat{y}_m)^2}}{\left(\sqrt{\frac{1}{n}\sum_{m=1}^{n} y_m^2} + \sqrt{\frac{1}{n}\sum_{m=1}^{n}\hat{y}_m^2}\right)} \tag{8}$$

$$\mathrm{MAD} = \sum_{m=1}^{n}|y_m - \hat{y}_m|, \tag{9}$$

$$RMSE = \sqrt{\frac{1}{n}\sum_{m=1}^{n}(y_m - \hat{y}_m)^2} \tag{10}$$

Table 1 Pseudocode of GAAS for finding weights of FMW-ANN.

```
Genetic Algorithms started
      Inputs:
            The chromosome with entries equal to weights of FMW-ANN as:
            W = [a,b,c] for a = [a_1,a_2,...,a_m], b = [b_1,b_2,...,b_m], and c = [c_1,c_2,...,c_m]
            Initial population based on n number of chromosome's W as:
            P = [W_1, W_2,,...,W_n]^t, for w_i = [a_i, b_i,...,c_i]^t
      Output:
            The best optimized weights for FMW-ANN by GA, W_Best-GA.
      Initialization
            Construct W with real bounded entries and set of W to form P. Set
            settings of 'GA' and 'gaoptimset' routines
      Fitness evaluation
            Obtained the E for each W in P by equations (5).
      Termination
            Terminate the for any of the following
            'Fitness'' E → 10^-15, Tolerances 'TolFun'→10^-20, 'TolCon'→10^-20,
            'StallGenLimit' →100. 'Generations'→75, 'PopulationSize'→ 300
            and default other.
            Go to step storage, when termination condition meets,
      Ranking
            Ranked each W of P on E given in equation (5).
      Reproduction
            Create new P using Selection, Crossover and Mutations routines
            '@selectionuniform','@crossoverheuristic'                   and
            '@mutationadaptfeasible', respectively. Four best ranked W of P
            for elitism:
            Go to 'fitness evaluation' step
      Storage
            Save W_Best-GA, E, with time, generation and function counts.
End Genetic algorithms
AS procedure Started
      Inputs
            The initial weights of GA, W_Best-GA
      Output
            The best weights for FMW-ANN by GAAS method, W_GAAS
      Initialize
            Initial weights of GAs, W_Best-GA, as a start point of the algorithm
            Set bounded, constraints limits, iterations and other
      Terminate
            Stop in case of
            'Fitness' E ≤ 10^-14, 'iterations'' = 700, tolerances 'TolFun' ≤
            10^-20, 'TolX' ≤ 10^-20, ''TolCon'' ≤ 10^-20, 'MaxFunEvals' ≤ 200000
and         default others
      While (Terminate conditions attained)
            Fitness calculation
                  Determined the fitness E by equations (5.
            Fine Tuning
                  Use 'fmincon' routine with algorithm 'active-set' for rapid
                  modification of W at each cycle.
                  Go to fitness calculation step with improved W
      End While loop
      Accumulate
            Store the W_GAAS, E, time, iterations and function counts.
ASA Procedure End
Dataset Generation
Repeat 100 times the GAAS procedure to create a dataset of the optimization
variables for FMW-ANN to solve NS-FLE system for effective statistical
inferences
```

where n represents the number of grid points. The optimal values of TIC, MAD and RMSE metrics are zeros in case of perfect modelling. The average values of The definitions of TIC, MAD and RMSE measures on the basis of sufficient large number of trials represents G-TIC, G-MAD), and G-RMSE, respectively. The optimal values of TIC, MAD and RMSE metrics as well as their global variant are zeros in case of perfect modelling.

4. Simulation and results

The results of detailed simulations for FMW-ANN-GAAS for solving NS-FLE equation is presented here for six different cases in order to evaluate the performance. The results of FMW-ANN-GAAS for all the six cases of NS-FLE model are presented with enough graphical and numerical illustrations to examine the accuracy and convergence.

Problem I:

Consider the NS-FLE differential equation (1) based system after multiplication denominator of second term both sides and homogeneous boundary condition by taking $c_o = d_0 = 0$ as:

$$x^{\alpha-\beta}D^{\alpha}y(x) + \lambda D^{\alpha}y(x) + x^{\alpha-\beta}f(x,y) = x^{\alpha-\beta}g(x), \tag{11}$$

$$y(0) = 0, \; y(1) = 0,$$

by substituting $l = \alpha - \beta$, $h(x,y) = x^{\alpha-\beta}f(x,y)$ and $j(x) = x^{\alpha-\beta}g(x)$, we have

$$x^{l}D^{\alpha}y(x) + \lambda D^{\alpha}y(x) + h(x,y) = j(x), \tag{12}$$

$$y(0) = 0, \; y(1) = 0,$$

the particular expressions used for functions $h(x,y)$ and $j(x)$ as:

$$h(x,y) = x^{2-\alpha}y(x) \tag{13}$$

$$j(x) = \left(\lambda + x^{l}\right)\left(\frac{\Gamma(p+1)}{\Gamma(p-\alpha+1)}x^{p-\alpha} - \frac{\Gamma(q+1)}{\Gamma(q-\alpha+1)}x^{q-\alpha}\right) + x^{p+\alpha} - x^{q+\alpha}$$

for positive integers p and q.

Using the relation in (13) in equation (12), we have

$$x^{l}D^{\alpha}y(x) + \lambda D^{\alpha}y(x) + \frac{1}{x^{\alpha-2}}y(x) = (\lambda + x^{l})\left(\frac{\Gamma(p+1)}{\Gamma(p-\alpha+1)}x^{p-\alpha} - \frac{\Gamma(q+1)}{\Gamma(q-\alpha+1)}x^{q-\alpha}\right) + x^{p-\alpha+2} - x^{q-\alpha+2}, \tag{14}$$

$$y(0) = 0, \; y(1) = 0,$$

the exact solution of the NS-FLE equation (14) is written as:

$$y(x) = x^{p} - x^{q} \tag{15}$$

Now for particular values of $p = 3$ and $q = 4$, NS-FLE equation (14) and its solution (15) are given as

$$x^{l}D^{\alpha}y(x) + \lambda D^{\alpha}y(x) + \frac{1}{x^{\alpha-2}}y(x) = (\lambda + x^{l})\left(\frac{6}{\Gamma(4-\alpha)}x^{3-\alpha} - \frac{2}{\Gamma(q-\alpha+1)}x^{2-\alpha}\right) + x^{5=\alpha} - x^{4-\alpha}, \tag{16}$$

$$y(0) = 0, \; y(1) = 0,$$

$$y(x) = x^{3} - x^{2}$$

The error based fitness function of equation (16) using equation (5) is given as:

$$E = \frac{1}{N}\sum_{i=1}^{m}\begin{pmatrix} x_m^{l}D^{\alpha}\hat{y}_m + \lambda D^{\alpha}\hat{y}_m + \frac{1}{x_m^{\alpha-2}} - x_m^{5-\alpha} + x_m^{4-\alpha} \\ -\left(\lambda + x_m^{l}\right)\left(\frac{6}{\Gamma(4-\alpha)}x_m^{3-\alpha} - \frac{2}{\Gamma(q-\alpha+1)}x_m^{2-\alpha}\right)\end{pmatrix}^2 + \frac{1}{2}\left((\hat{y}_0)^2 + (\hat{y}_m)^2\right) \tag{17}$$

Six cases of NS-FLE system (11) are considered by taking different values of α, l and λ as listed in Table 2.

Optimization variables of FMW-ANN, to analyze all six variants of NS-FLE system (16), is conducted with the combination of global and local search strength of GAAS as per procedure listed in pseudocode given in Table 1. The whole procedure listed in Table 1 is repeated for hundred number of runs to create a large dataset for FMW-ANN operatiions. The mathematical relations derived by one set of optimized parameters, as shown in Fig. 1, of FMW-ANN by GAAS technique for each case of NS-FLE system are given as:

$$\begin{gathered}\hat{y}_{C-1} = 0.3092\\ \left(35(0.5439x - 0.0916)^4 - 84(0.5439x - 0.0916)^5 + 70(0.5439x - 0.0916)^6 - 20(0.5439x - 0.0916)^7\right)\\ -0.4219\\ \left(35(0.0499x - 0.0930)^4 - 84(0.0499x - 0.0930)^5 + 70(0.0499x - 0.0930)^6 - 20(0.0499x - 0.0930)^7\right)\\ +\ldots + 1.0940\\ \left(35(0.2980x - 0.1071)^4 - 84(0.2980x - 0.1071)^5 + 70(0.2980x - 0.1071)^6 - 20(0.2980x - 0.1071)^7\right),\end{gathered} \tag{18}$$

$$\begin{gathered}\hat{y}_{C-2} = 0.7889\\ \left(35(0.5916x + 0.7570)^4 - 84(0.5916x + 0.7570)^5 + 70(0.5916x + 0.7570)^6 - 20(0.5916x + 0.7570)^7\right)\\ +0.3089\\ \left(35(-0.6838x + 0.2450)^4 - 84(-0.6838x + 0.2450)^5 + 70(-0.6838x + 0.2450)^6 - 20(-0.6838x + 0.2450)^7\right)\\ +\ldots - 0.9791\\ \left(35(0.0210x + 0.8873)^4 - 84(0.0210x + 0.8873)^5 + 70(0.0210x + 0.8873)^6 - 20(0.0210x + 0.8873)^7\right),\end{gathered} \tag{19}$$

Table 2 Variants of NS-FLE system.

Index	Parameteric values		
	α	l	λ
Case-1	1.2	0.7	1
Case-2	1.5	1	1
Case-3	1.8	1.3	1
Case-4	1.2	0.7	3
Case-5	1.5	1	3
Case-6	1.8	1.3	3

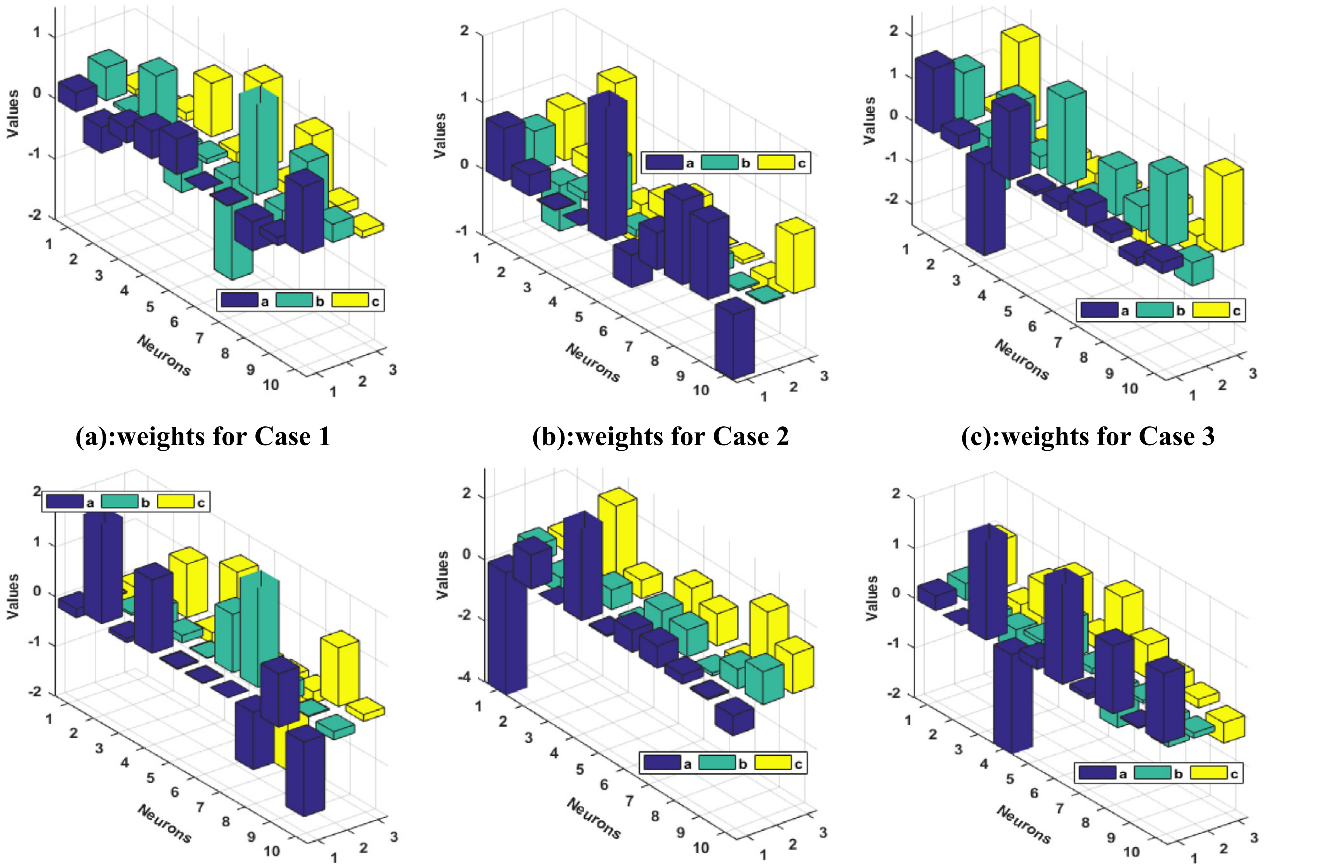

(a):weights for Case 1 (b):weights for Case 2 (c):weights for Case 3

(d):weights for Case 4 (e):weights for Case 5 (f):weights for Case 6

Fig. 1 Set of trained weight vectors of FMW-ANN for cases 1 to 6 of NS-FLE system.

$$\begin{aligned}\hat{y}_{C-3} = {} & 1.5378\left(35(1.1811x-0.0566)^4-84(1.1811x-0.0566)^5+70(1.1811x-0.0566)^6-20(1.1811x-0.0566)^7\right)\\ & -0.3133\left(35(-1.3617x+2.0217)^4-84(-1.3617x+2.0217)^5+70(-1.3617x+2.0217)^6-20(-1.3617x+2.0217)^7\right)\\ & +\ldots+0.2656\left(35(-0.5513x+1.7973)^4-84(-0.5513x+1.7973)^5+70(-0.5513x+1.7973)^6-20(-0.5513x+1.7973)^7\right),\end{aligned} \tag{20}$$

$$\begin{aligned}\hat{y}_{C-4} = {} & -0.1797\left(35(-0.0208x-0.09161)^4-84(-0.0208x-0.09161)^5+70(-0.0208x-0.09161)^6-20(-0.0208x-0.09161)^7\right)\\ & +2.5514\left(35(-0.0415x-0.1137)^4-84(-0.0415x-0.1137)^5+70(-0.0415x-0.1137)^6-20(-0.0415x-0.1137)^7\right)\\ & +\ldots-1.4951\left(35(-0.1646x+0.1344)^4-84(-0.1646x+0.1344)^5+70(-0.1646x+0.1344)^6-20(-0.1646x+0.1344)^7\right),\end{aligned} \tag{21}$$

$$\begin{aligned}\hat{y}_{C-5} = & -8.0125\left(35(0.5327x+0.4259)^4-84(0.5327x+0.4259)^5+70(0.5327x+0.4259)^6-20(0.5327x+0.4259)^7\right)\\ & +1.1136\left(35(-0.5186x-0.5861)^4-84(-0.5186x-0.5861)^5+70(-0.5186x-0.5861)^6-20(-0.5186x-0.5861)^7\right)\\ & +\ldots-0.6563\left(35(1.0788x+1.2783)^4-84(1.0788x+1.2783)^5+70(1.0788x+1.2783)^6-20(1.0788x+1.2783)^7\right),\end{aligned} \tag{22}$$

$$\begin{aligned}\hat{y}_{C-6} = & \,0.2908\left(35(0.3358x-0.9622)^4-84(0.3358x-0.9622)^5+70(0.3358x-0.9622)^6-20(0.3358x-0.9622)^7\right)\\ & +0.0007\left(35(0.2163x-1.0749)^4-84(0.2163x-1.0749)^5+70(0.2163x-1.0749)^6-20(0.2163x-1.0749)^7\right)\\ & +\ldots+1.4015\left(35(-0.1081x-0.4119)^4-84(-0.1081x-0.4119)^5+70(-0.1081x-0.4119)^6-20(-0.1081x-0.4119)^7\right),\end{aligned} \tag{23}$$

The approximate solutions$\hat{y}(x)$are determined by equations. (18–23) and outcomes are graphically illustrated in Fig. 2 and numerically in Table 3 along with reference exact solution for each case of NS-FLE equation (16). The exact and proposed results of FMW-ANN-GAAS overlap for all six cases of NS-FLE equation. To analyse the matching order of the results, the absolute error (AE) from exact solutions are calculated for all six cases NS-FLE equation and outcomes are plotted in Fig. 2 and tabulated in Table 4. To performance indices of TIC, MAD, RMSE and fitness as indicated in equations (8), (9), (10) and (17) are calculated and result are provided graphically in Fig. 3 for each case. All these illustrations evidently show that FMW-ANN-GAAS solutions are in a good agreement with the reference exact solutions in all six cases of NS-FLE equation. Near optimum values are obtained for each the performance metric that further established the worth of the proposed FMW-ANN-GAAS scheme.

The analysis of the performance of FMW-ANN-GAAS to solve NS-FLE system (16) is conducted through statistics and results are presented in Figs. 4 to 9 and tables 5 to 10 for 100 independent executions.

Statistical results by means of minimum (Min), Maximum (Max), median (Med), and semi interquartile range (SIR), i.e., SIR is basically one half of the difference of 3rdquartile (Q_3 = 75% data) and 1stquartile (Q_1 = 25% data), are calculated for 100 executions of FMW-ANN-GAAS to solve all six cases of NS-FLE equation (16). These statistical observations are used for precision analysis of presented FMW-ANN-GAAS technique. The independent execution of the algorithm with parameter of FWM-ANN attaining the MIN and MAX error based fitness value is called the best and worst run, respectively. The results of NS-FLE equation for the best, mean and exact solution are plotted in Fig. 4, while the values of AE for the best, worst and mean are tabulated in Fig. 5. The best AE values lie between the ranges of 10^{-07} to 10^{-10} while, the reasonably accuracy of mean values for each case of the NS-FLE equation. The statistics by means of Min, Max, Med and SIR operator are tabulated in tables 5, 6 and 7 for cases (1–2), (3–4) and (5–6) of NS-FLE equation (16), respectively. It is clear that the scale of Min values lies around 10^{-08} to 10^{-09} which Max values also lies in good ranges for each case of NS-FLE model. Similarly, the median values also showed good results and lie around 10^{-04} to 10^{-05}. Finally, the SIR values lie around 10^{-03} to 10^{-05} that indicates very good ranges for each case of NS-FLE model.

The result of statistics in terms of fitness, MAD, RMSE and TIC gauges are plotted in Figs. 6, 7, 8 and 9, respectively for all six cases of NS-FLE equation (16). The histograms illustrations are used to find the tendency or trend of the results of fitness, MAD, RMSE and TIC, and are also provided for in Figs. 6 to 9, respectively. One may clearly understand that over 80% of independent implementations of FMW-ANN-GAAS obtained very good fitness, MAD, RMSE and TIC gauges for each case of NS-FLE system. All these results represent that over 80% of the runs of FMW-ANN-GAAS attained precise values of each performance measures.

To measure the convergence statistics of proposed FMW-ANN-GAAS scheme, the analysis on the basis of all four performance measures are tabulated in Table 8 for all six cases of NS-FLE system. It is clear, that most of runs obtained the levels 'FIT $\leq 10^{-03}$', 'MAD $\leq 10^{-03}$', 'RMSE $\leq 10^{-04}$' and 'TIC $\leq 10^{-07}$', while, the reasonable independent trails of FMW-ANN-GA can achieved relatively stiffer levels. Although, for higher precision levels, comparatively number of runs decreased considerably of the present FMW-ANN-GAAS scheme to fulfil the conditions. The convergence analysis of FMW-ANN-GAAS is further conducted on global performance operators based on G-FIT, G-MAD, G-RMSE and G-TIC and these results for 100 runs are tabulated in Table 9. The G-FIT, G-MAD, G-RMSE and G-TIC values lie around 10^{-02} to 10^{-04}, 10^{-02} to 10^{-03}, 10^{-02} to 10^{-03} and 10^{-06} to 10^{-07}, respectively, together with small standard deviation (SD) values. The close to optimal values of these global indices further validate the precision of the presented FMW-ANN-GAAS scheme.

The computational cost of the presented FMW-ANN-GAAS algorithm are examined through completed iterations/-cycles, average time of parameter adaptation and executed function counts during the process of find the decision variable of the networks. Complexity analysis for each case of NS-FLE

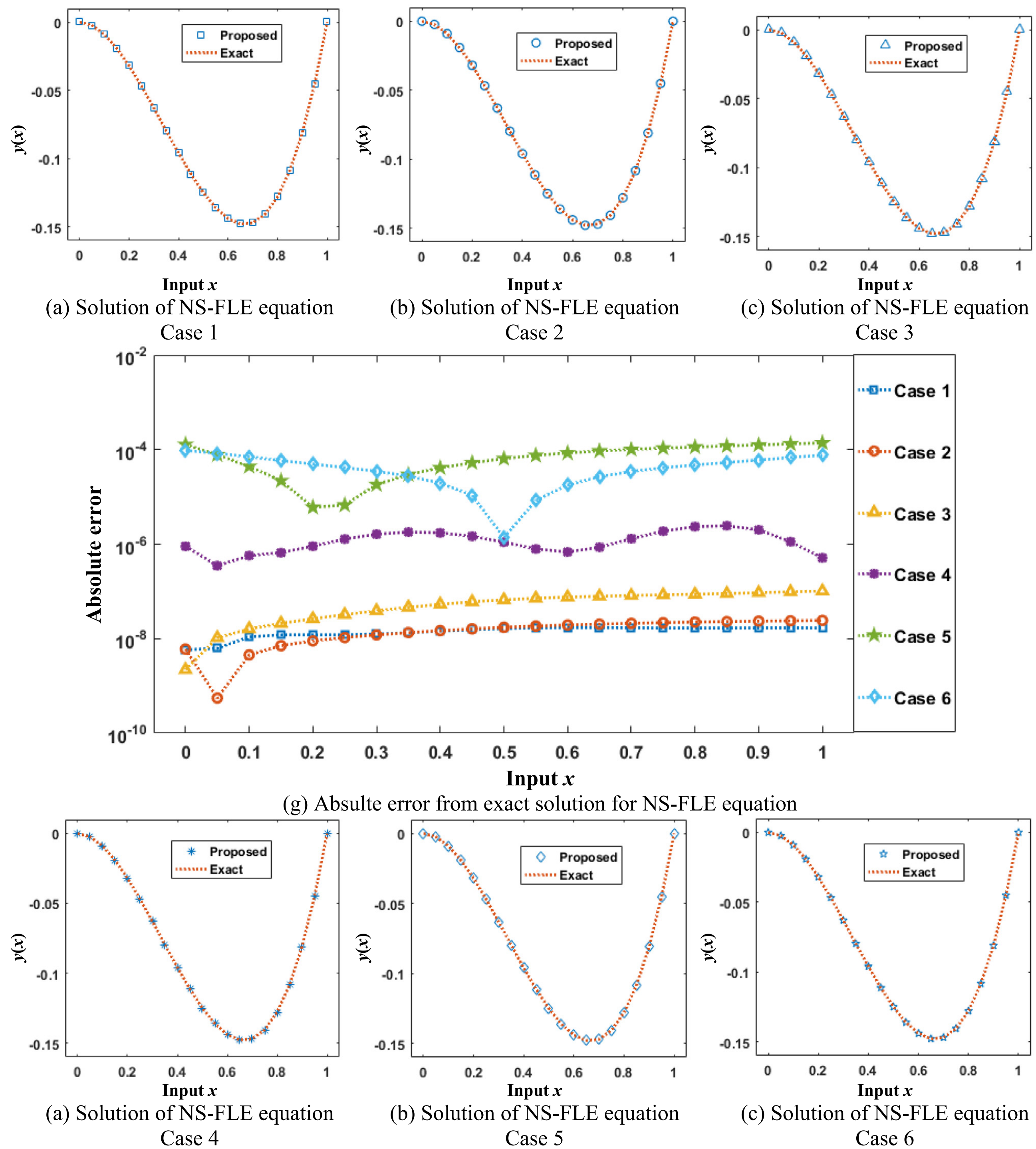

Fig. 2 Comparison of results of FMW-ANN-GAAS from exact solution for all six case of the NS-FLE system.

model are determined and the outcomes are listed in Table 10. One may observe that the average generations/iterations, time and evaluations of functions are around 212.95, 537.74 and 48888.28, for all six cases of NS-FLE system, respectively. These values are given to compare the efficiency of the proposed FMW-ANN-GAAS scheme.

5. Conclusions

A new stochastic computational solver FMW-ANN-GASA based on fractional Meyer wavelet artificial neural network optimized with integrated strength of genetic algorithm aid

Table 3 Results of FMW-ANN-GAAS and exact solution for each variant of NS-FLE system.

x	Exact Solution$y(x)$	Approximate Solution$\hat{y}(x)$					
		Case-1	Case-2	Case-3	Case-4	Case-5	Case-6
0	0.000000000	−0.000000009	−0.000000006	0.000000066	−0.000000002	−0.000000055	−0.000000051
0.05	−0.002375000	−0.002374999	−0.002374999	−0.002374946	−0.002375001	−0.002375040	−0.002375047
0.1	−0.009000000	−0.008999992	−0.008999995	−0.008999962	−0.009000000	−0.009000031	−0.009000043
0.15	−0.019125000	−0.019124988	−0.019124993	−0.019124978	−0.019125000	−0.019125025	−0.019125040
0.2	−0.032000000	−0.031999988	−0.031999991	−0.031999990	−0.032000000	−0.032000020	−0.032000037
0.25	−0.046875000	−0.046874991	−0.046874989	−0.046874998	−0.046875000	−0.046875016	−0.046875034
0.3	−0.063000000	−0.062999994	−0.062999988	−0.063000003	−0.062999999	−0.063000013	−0.063000031
0.35	−0.079625000	−0.079624996	−0.079624987	−0.079625005	−0.079624999	−0.079625009	−0.079625028
0.4	−0.096000000	−0.095999997	−0.095999985	−0.096000006	−0.095999998	−0.096000005	−0.096000026
0.45	−0.111375000	−0.111374997	−0.111374984	−0.111375008	−0.111374998	−0.111375001	−0.111375023
0.5	−0.125000000	−0.124999995	−0.124999983	−0.125000009	−0.124999998	−0.124999998	−0.125000021
0.55	−0.136125000	−0.136124994	−0.136124982	−0.136125011	−0.136124999	−0.136124995	−0.136125018
0.6	−0.144000000	−0.143999992	−0.143999981	−0.144000014	−0.143999998	−0.143999992	−0.144000016
0.65	−0.147875000	−0.147874992	−0.147874980	−0.147875016	−0.147874998	−0.147874990	−0.147875013
0.7	−0.147000000	−0.146999994	−0.146999979	−0.147000018	−0.146999997	−0.146999988	−0.147000011
0.75	−0.140625000	−0.140624996	−0.140624978	−0.140625020	−0.140624996	−0.140624986	−0.140625008
0.8	−0.128000000	−0.127999999	−0.127999978	−0.128000021	−0.127999996	−0.127999984	−0.128000006
0.85	−0.108375000	−0.108375001	−0.108374977	−0.108375023	−0.108374996	−0.108374981	−0.108375003
0.9	−0.081000000	−0.081000002	−0.080999977	−0.081000026	−0.080999996	−0.080999979	−0.081000001
0.95	−0.045125000	−0.045125000	−0.045124976	−0.045125029	−0.045124998	−0.045124976	−0.045124999
1	0.000000000	0.000000002	0.000000024	−0.000000034	0.000000001	0.000000026	0.000000003

Table 4 Comparison of FMW-ANN-GAAS results on the basis of absolute error form exact solutions for each case of NS-FLE system.

x	Absolute Error$\lvert y(x) - \hat{y}(x)\rvert$					
	Case-1	Case-2	Case-3	Case-4	Case-5	Case-6
0	8.817E-09	6.010E-09	6.581E-08	1.829E-09	5.512E-08	5.136E-08
0.05	8.001E-10	5.541E-10	5.427E-08	5.155E-10	4.041E-08	4.677E-08
0.1	8.187E-09	4.536E-09	3.766E-08	4.287E-10	3.119E-08	4.315E-08
0.15	1.167E-08	7.101E-09	2.204E-08	4.212E-10	2.503E-08	3.999E-08
0.2	1.161E-08	8.966E-09	1.001E-08	1.200E-10	2.039E-08	3.701E-08
0.25	9.356E-09	1.054E-08	2.051E-09	4.334E-10	1.637E-08	3.412E-08
0.3	6.429E-09	1.201E-08	2.546E-09	1.038E-09	1.253E-08	3.127E-08
0.35	4.077E-09	1.344E-08	4.948E-09	1.496E-09	8.721E-09	2.848E-08
0.4	3.012E-09	1.484E-08	6.320E-09	1.703E-09	4.966E-09	2.576E-08
0.45	3.354E-09	1.616E-08	7.549E-09	1.674E-09	1.369E-09	2.314E-08
0.5	4.714E-09	1.737E-08	9.127E-09	1.529E-09	1.956E-09	2.059E-08
0.55	6.384E-09	1.847E-08	1.117E-08	1.441E-09	4.935E-09	1.810E-08
0.6	7.569E-09	1.944E-08	1.350E-08	1.574E-09	7.555E-09	1.563E-08
0.65	7.637E-09	2.030E-08	1.583E-08	2.018E-09	9.868E-09	1.317E-08
0.7	6.328E-09	2.107E-08	1.789E-08	2.741E-09	1.199E-08	1.070E-08
0.75	3.882E-09	2.176E-08	1.959E-08	3.567E-09	1.406E-08	8.231E-09
0.8	1.038E-09	2.240E-08	2.111E-08	4.198E-09	1.623E-08	5.795E-09
0.85	1.139E-09	2.297E-08	2.290E-08	4.301E-09	1.859E-08	3.434E-09
0.9	1.649E-09	2.348E-08	2.552E-08	3.661E-09	2.116E-08	1.184E-09
0.95	2.096E-10	2.391E-08	2.935E-08	2.429E-09	2.381E-08	9.623E-10
1	1.777E-09	2.429E-08	3.409E-08	1.477E-09	2.620E-08	3.110E-09

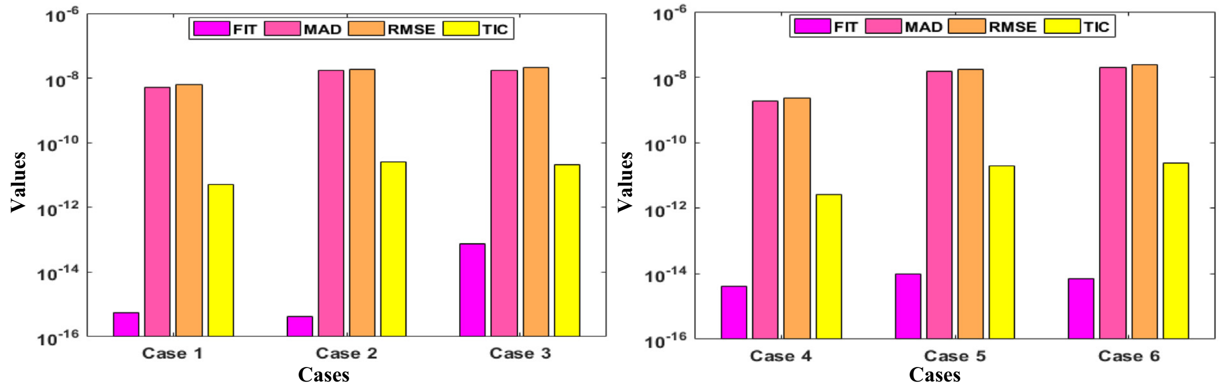

(a) NS-FLE equation for Cases 1-3 (b) NS-FLE equation for Cases 4-6

Fig. 3 The magnitude of performance indices for each case of NS-FLE system.

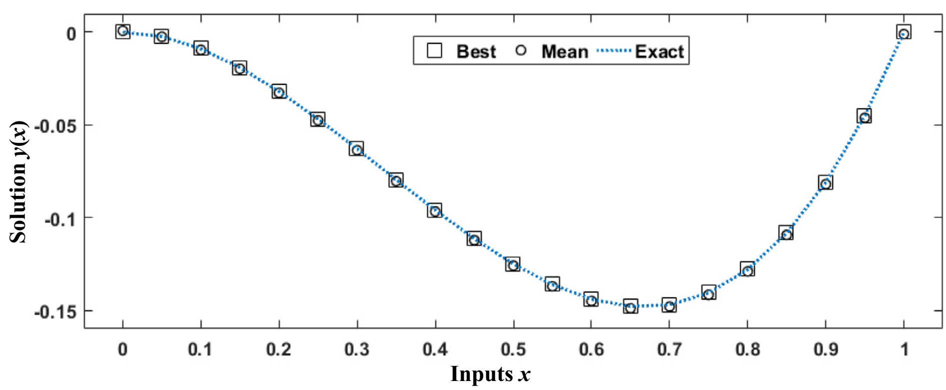

Fig. 4 Statistical operators based comparison of results through exact solutions for case 1 of NS-FLE system.

with active-set method is presented for reliable and effective numerical treatment for nonlinear singular fractional Lane-Emden differential equation. The proposed FMW-ANN-GASA methodology is viably implemented on fractional Lane-Emden system for six different scenarios to prove its accuracy, convergence, stability and robustness. Comparison of the proposed numerical solutions of FMW-ANN-GASA with exact solutions shows the matching of order 7 to 10 decimal places of accuracy which verify its correctness and efficacy. Statistical measures of the present results indicate that more than 75% runs of the algorithm give precise results consistently. Consequently, the present technique is not only effective but one can implement easily too. The proposed FMW-ANN-GAAS is a fast convergent procedure that can implemented to solve the linear/nonlinear, singular/nonsingular systems governed with differential equation.

In future, one may exploit the FMW-ANN-GASA scheme for solution of fractional order systems represented with nonlinear Riccati equation, Baglay-Torvik equation, Van-der Pol system and Painleve eqautions.

Declaration of Competing Interest

The authors declare that they have no known competing financial interests or personal relationships that could have

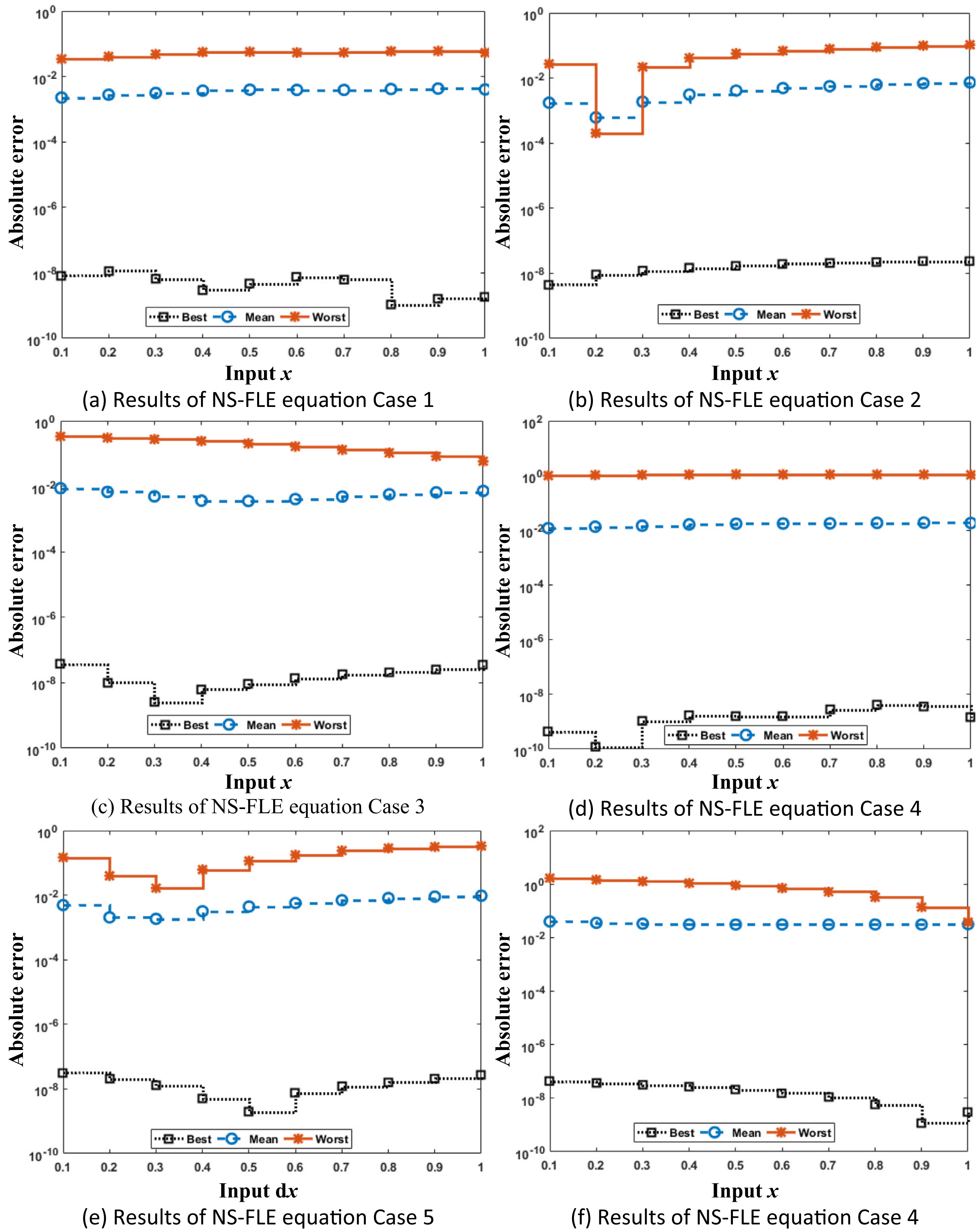

Fig. 5 Statistical operators based comparison through magnitude of AE for all six cases of NS-FLE system.

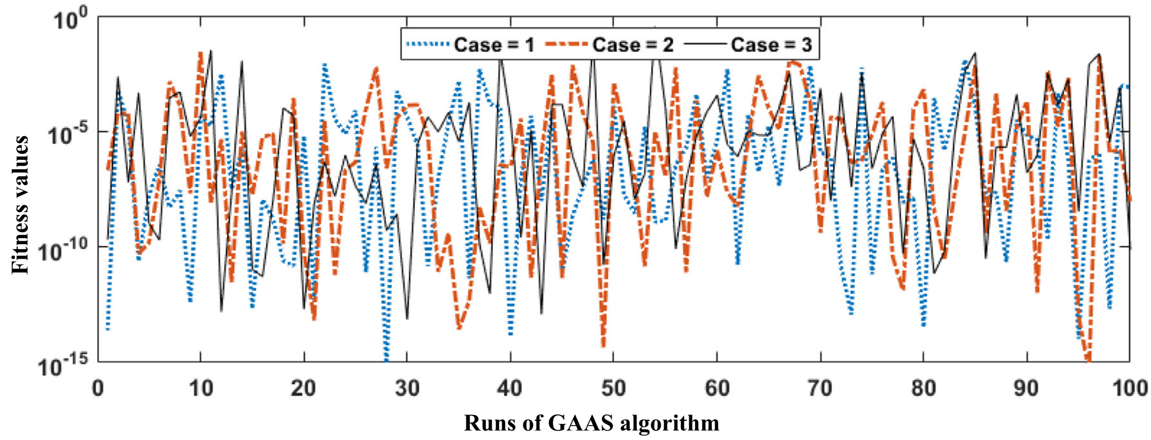

(a) Fitness analysis for Cases 1 to 3 of NS-FLE equation

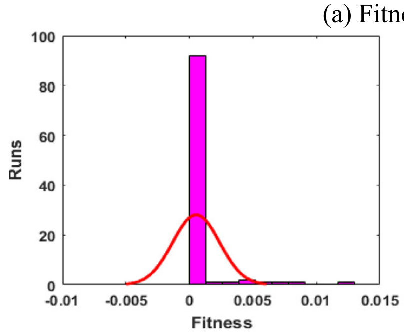

(c): Case 1 histogram

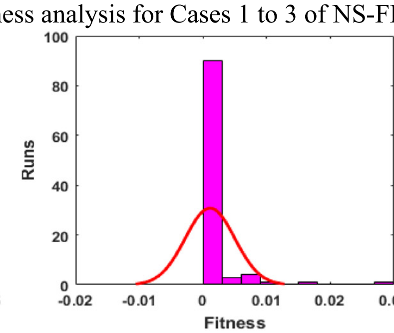

(d): Case 2 histogram

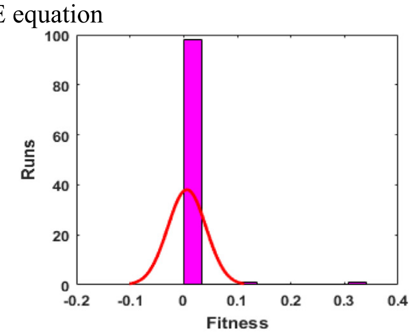

(e): Case 3 histogram

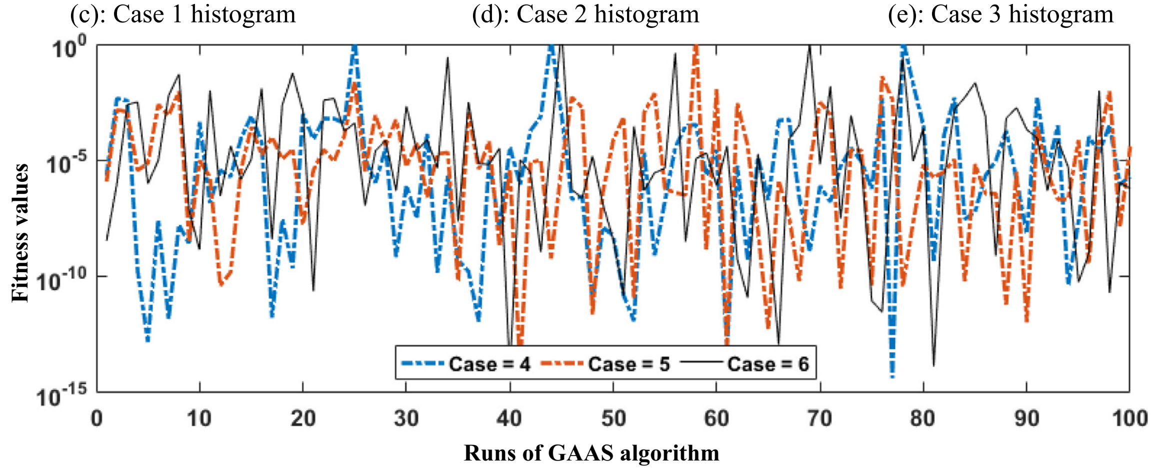

(b) Fitness analysis for Cases 4 to 6 of NS-FLE equation

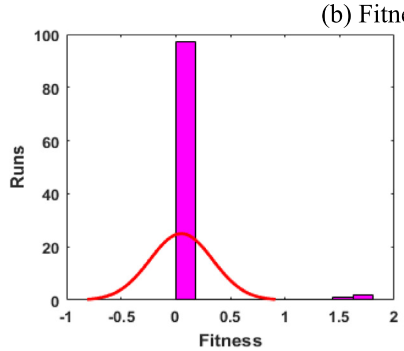

(f): Case 4 histogram

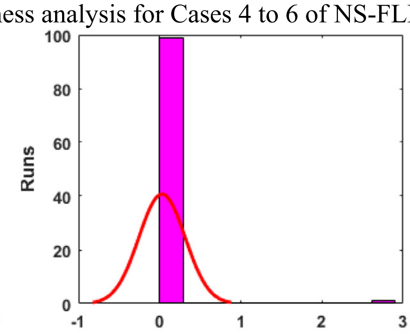

(g): Case 5 histogram

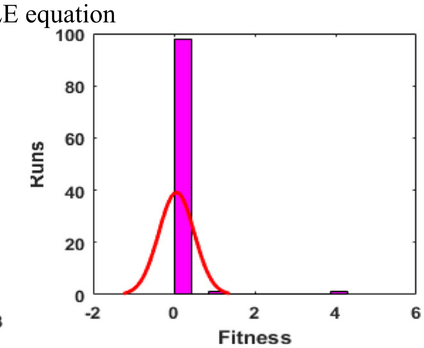

(h): Case 6 histogram

Fig. 6 Comparison of results through fitness gauge of GAAS method for all six cases of NS-FLE system.

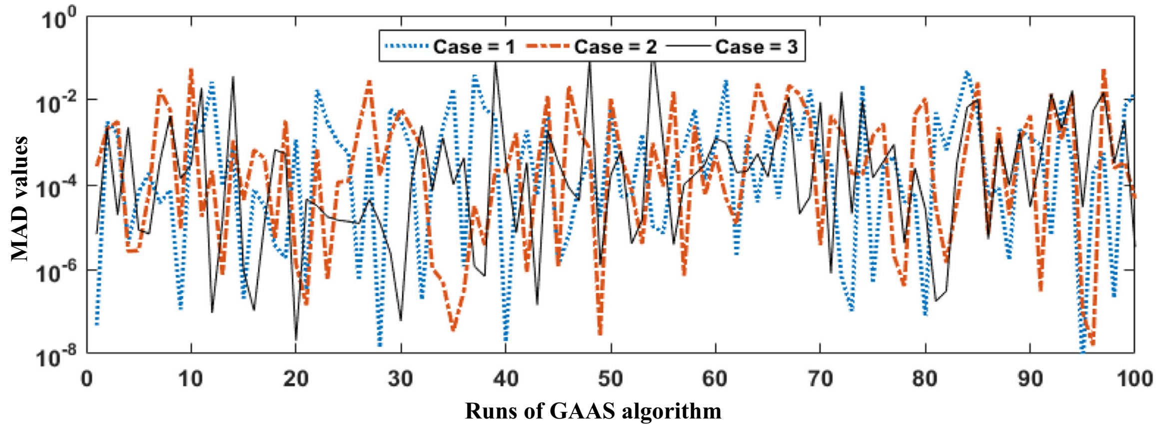

(a) MAD analysis for Cases 1 to 3 of NS-FLE equation

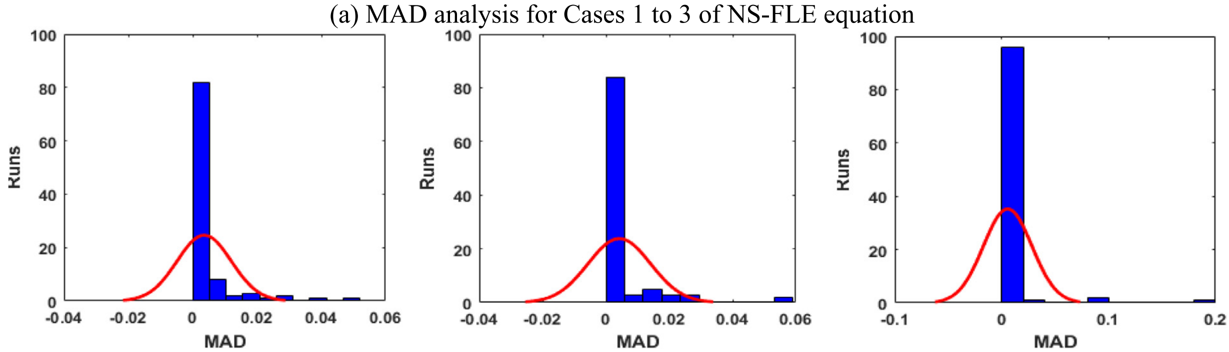

(c): Case 1 histogram (d): Case 2 histogram (e): Case 3 histogram

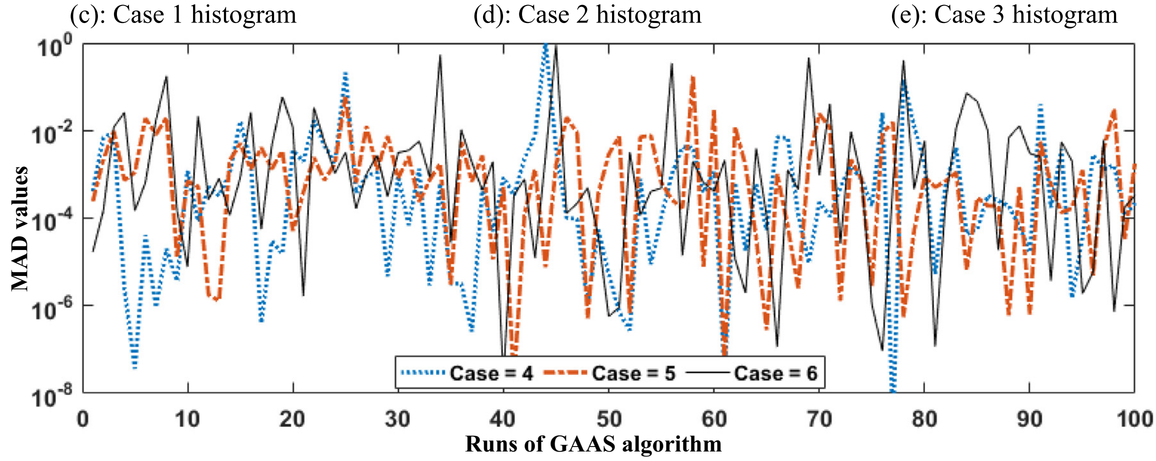

(b) MAD analysis for Cases 4 to 6 of NS-FLE equation

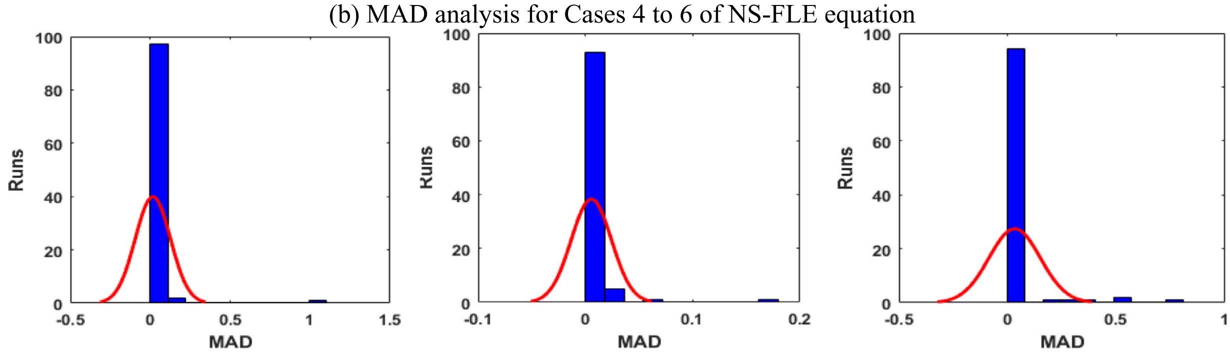

(f): Case 4 histogram (g): Case 5 histogram (h): Case 6 histogram

Fig. 7 Comparison of results through MAD gauge of GAAS method for all six cases of NS-FLE system.

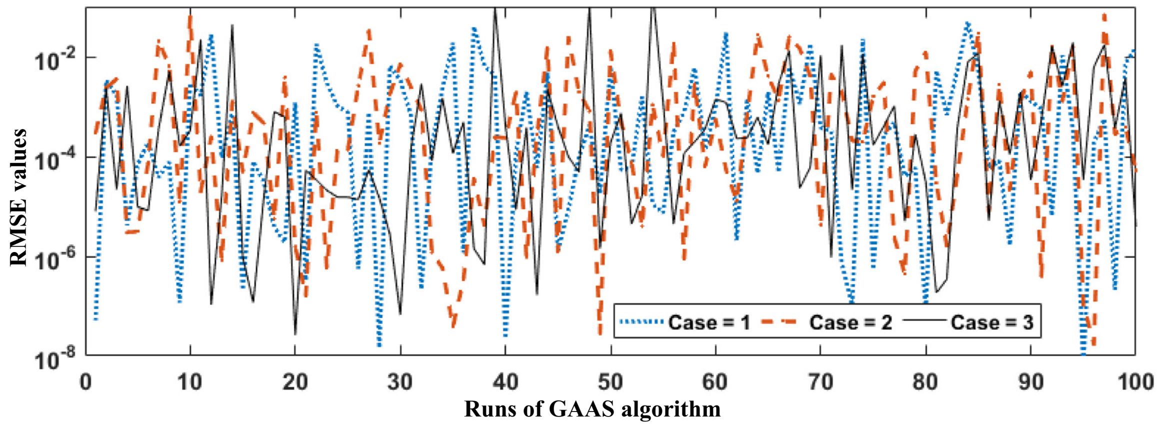

(a) RMSE analysis for Cases 1 to 3 of NS-FLE equation

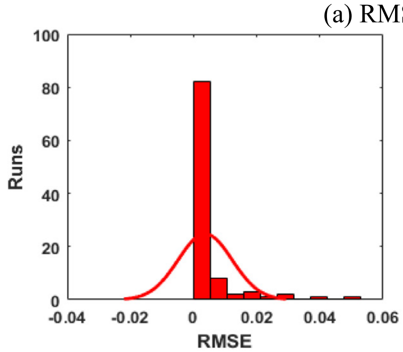

(c): Case 1 histogram

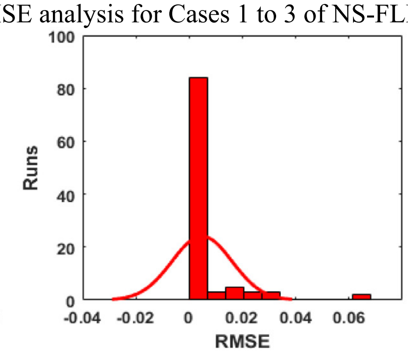

(d): Case 2 histogram

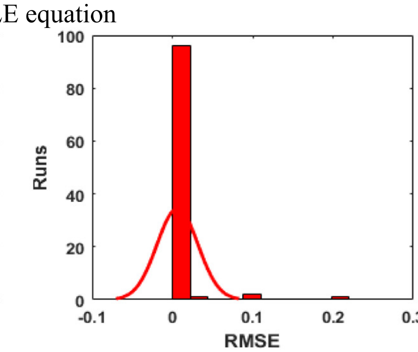

(e): Case 3 histogram

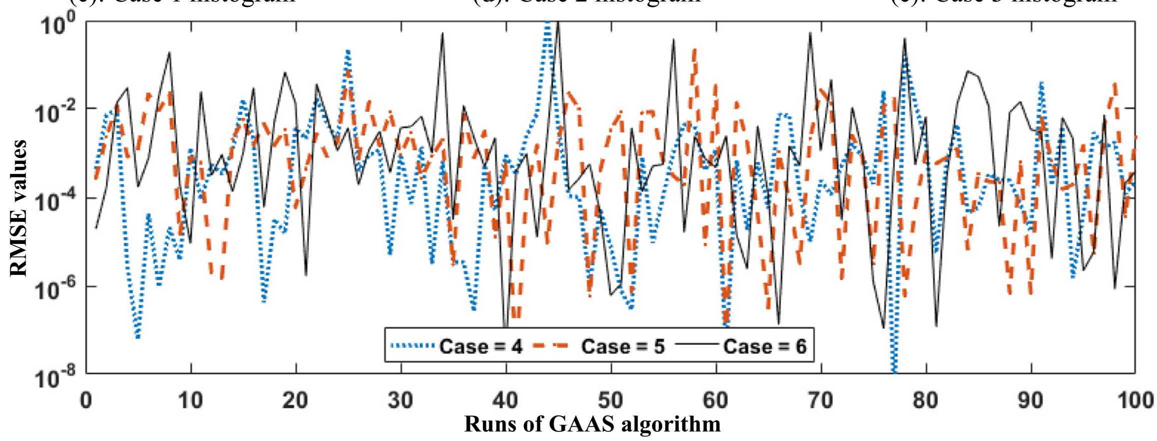

(b) RMSE analysis for Cases 1 to 3 of NS-FLE equation

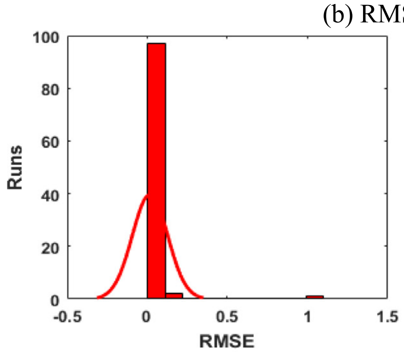

(f): Case 4 histogram

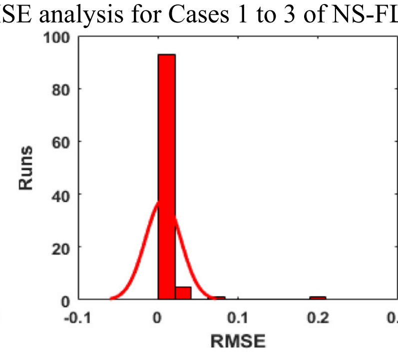

(g): Case 5 histogram

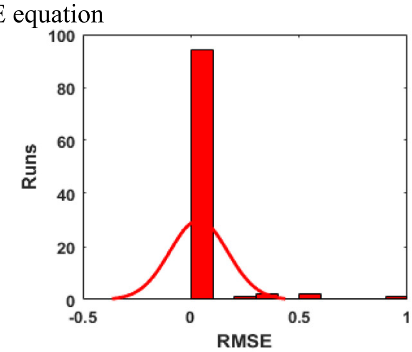

(h): Case 6 histogram

Fig. 8 Comparison of results through RMSE gauge of GAAS method for all six cases of NS-FLE system.

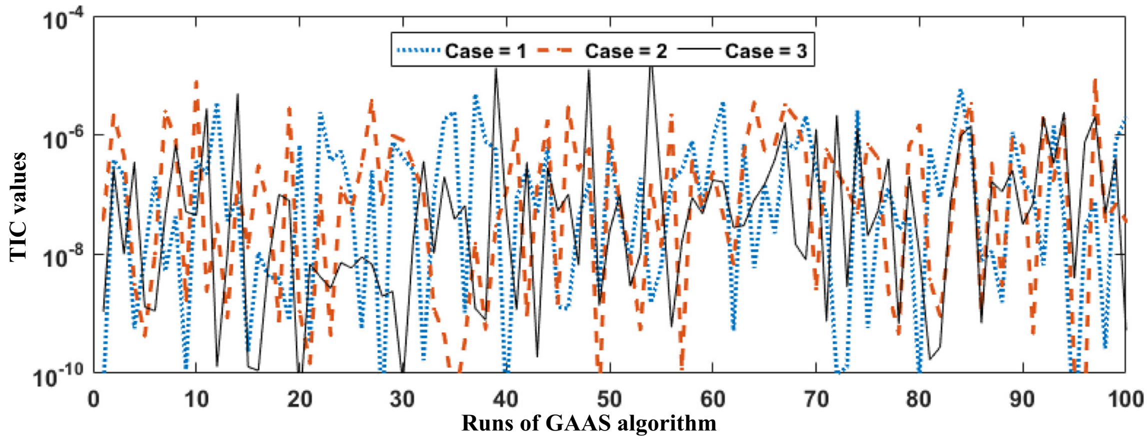

(a) Fitness analysis for Cases 1 to 3 of NS-FLE equation

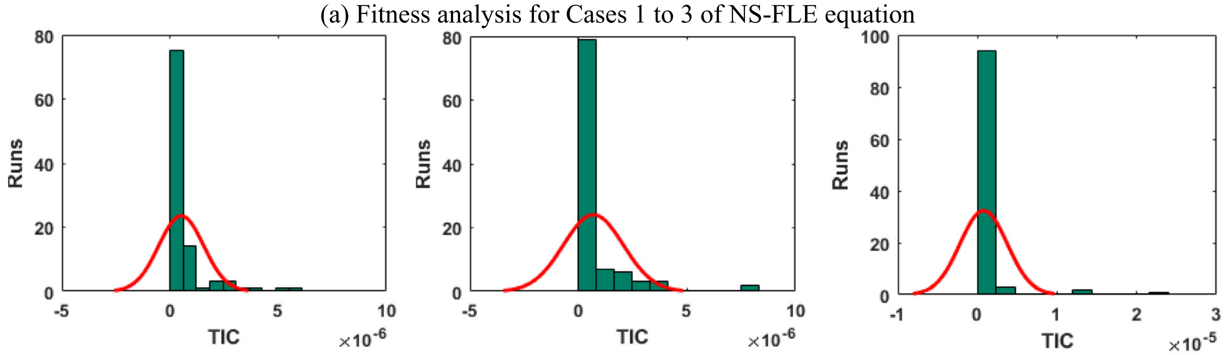

(c): Case 1 histogram (d): Case 2 histogram (e): Case 3 histogram

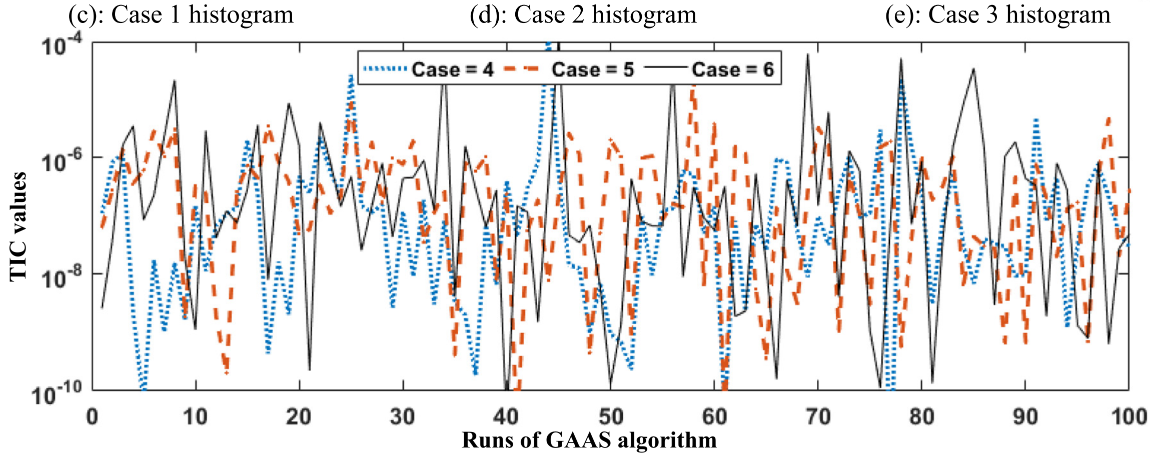

(b) TIC analysis for Cases 1 to 3 of NS-FLE equation

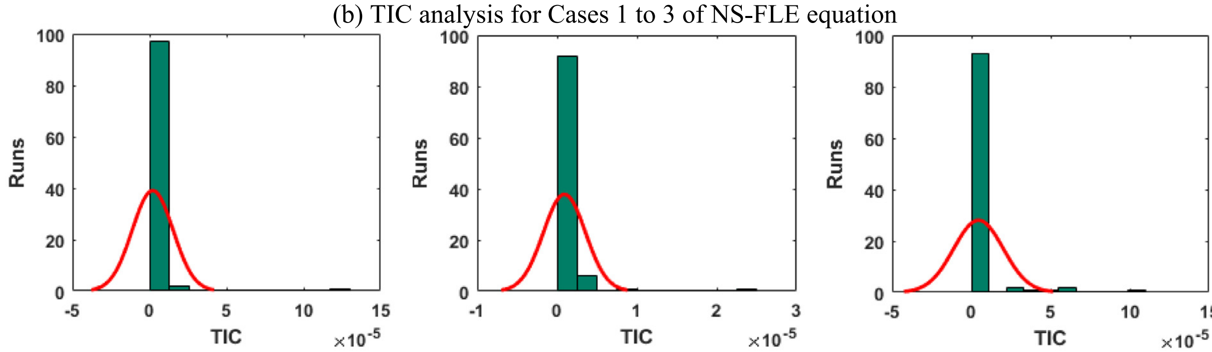

(f): Case 4 histogram (g): Case 5 histogram (h): Case 6 histogram

Fig. 9 Comparison of results through TIC gauge of GAAS method for all six cases of NS-FLE system.

Table 5 Comparison on different statistical metrics for FMW-ANN-GAAS results for cases 1 and 2 of NS-FLE system.

x	Case 1				Case 2			
	Min	Max	Median	SIR	Min	Max	Med	SIR
0.1	8.187E-09	3.428E-02	1.892E-04	6.859E-04	3.332E-09	2.719E-02	1.299E-04	6.724E-04
0.2	1.161E-08	4.095E-02	2.455E-04	8.612E-04	6.946E-10	1.174E-02	1.306E-05	6.821E-05
0.3	6.429E-09	4.782E-02	2.808E-04	1.111E-03	9.438E-10	2.515E-02	1.248E-04	5.564E-04
0.4	3.012E-09	5.554E-02	3.653E-04	1.348E-03	9.053E-09	4.364E-02	2.301E-04	1.004E-03
0.5	4.714E-09	5.690E-02	3.834E-04	1.461E-03	1.706E-08	5.699E-02	2.969E-04	1.302E-03
0.6	7.569E-09	5.390E-02	3.644E-04	1.390E-03	1.944E-08	6.840E-02	3.461E-04	1.548E-03
0.7	6.328E-09	5.397E-02	3.646E-04	1.400E-03	2.107E-08	7.844E-02	3.974E-04	1.718E-03
0.8	1.038E-09	5.888E-02	4.019E-04	1.469E-03	2.240E-08	8.904E-02	4.579E-04	1.823E-03
0.9	1.649E-09	5.999E-02	4.157E-04	1.520E-03	2.348E-08	9.854E-02	5.088E-04	1.983E-03
1.0	1.777E-09	5.339E-02	3.712E-04	1.437E-03	2.429E-08	1.046E-01	5.337E-04	2.266E-03

Table 6 Comparison on different statistical metrics for FMW-ANN-GAAS results for cases 3 and 4 of NS-FLE system.

x	Case 3				Case 4			
	Min	Max	Median	SIR	Min	Max	Med	SIR
0.1	1.611E-08	3.357E-01	1.802E-04	8.486E-04	4.287E-10	1.003E + 00	2.076E-04	4.345E-04
0.2	1.001E-08	3.035E-01	1.209E-04	6.406E-04	1.200E-10	1.049E + 00	2.718E-04	5.604E-04
0.3	2.546E-09	2.755E-01	4.835E-05	2.403E-04	1.038E-09	1.063E + 00	3.290E-04	6.130E-04
0.4	3.245E-09	2.430E-01	4.773E-05	1.977E-04	1.703E-09	1.091E + 00	3.658E-04	8.077E-04
0.5	9.127E-09	2.043E-01	1.054E-04	4.056E-04	1.529E-09	1.106E + 00	3.964E-04	9.960E-04
0.6	1.350E-08	1.648E-01	1.238E-04	5.506E-04	1.574E-09	1.100E + 00	4.024E-04	1.107E-03
0.7	1.789E-08	1.314E-01	1.500E-04	6.515E-04	2.741E-09	1.094E + 00	4.107E-04	1.068E-03
0.8	2.111E-08	1.322E-01	1.972E-04	7.530E-04	4.198E-09	1.098E + 00	4.256E-04	9.845E-04
0.9	2.552E-08	1.568E-01	2.446E-04	8.626E-04	3.661E-09	1.093E + 00	4.492E-04	1.084E-03
1.0	3.409E-08	1.816E-01	2.298E-04	9.549E-04	1.477E-09	1.062E + 00	4.522E-04	1.240E-03

Table 7 Comparison on different statistical metrics for FMW-ANN-GAAS results for cases 5 and 6 of NS-FLE system.

x	Case 5				Case 6			
	Min	Max	Median	SIR	Min	Max	Med	SIR
0.1	3.119E-08	1.473E-01	5.108E-04	1.279E-03	4.315E-08	1.673E + 00	8.469E-04	3.366E-03
0.2	2.039E-08	4.150E-02	1.147E-04	4.117E-04	3.701E-08	1.453E + 00	6.651E-04	2.433E-03
0.3	9.803E-09	3.636E-02	2.151E-04	6.737E-04	3.127E-08	1.259E + 00	3.956E-04	1.573E-03
0.4	4.966E-09	6.164E-02	4.865E-04	1.086E-03	1.364E-08	1.075E + 00	6.775E-05	5.810E-04
0.5	1.956E-09	1.143E-01	6.772E-04	1.144E-03	4.839E-09	8.914E-01	2.936E-04	1.502E-03
0.6	7.555E-09	1.760E-01	7.856E-04	1.436E-03	1.563E-08	7.030E-01	4.919E-04	2.144E-03
0.7	1.199E-08	2.373E-01	9.630E-04	1.713E-03	1.070E-08	6.616E-01	7.269E-04	3.076E-03
0.8	1.623E-08	2.851E-01	1.104E-03	2.011E-03	5.795E-09	7.684E-01	8.869E-04	4.037E-03
0.9	2.116E-08	3.131E-01	1.247E-03	2.276E-03	1.184E-09	8.719E-01	1.087E-03	4.880E-03
1.0	2.620E-08	3.327E-01	1.375E-03	2.400E-03	3.110E-09	9.672E-01	1.266E-03	5.607E-03

Table 8 Convergence analysis for cases (1–6) of fractional Lane-Emden model.

Case	FIT≤			MAD ≤			RMSE≤			TIC ≤		
	10^{-03}	10^{-04}	10^{-05}	10^{-03}	10^{-04}	10^{-05}	10^{-04}	10^{-05}	10^{-06}	10^{-06}	10^{-07}	10^{-08}
1	96	88	76	81	55	31	55	31	21	99	46	26
2	92	85	70	83	54	35	53	33	23	98	43	29
3	92	84	69	85	66	41	65	39	16	97	53	27
4	97	85	71	85	53	34	51	34	21	98	40	25
5	94	78	67	76	52	30	51	29	18	96	41	25
6	86	72	58	76	47	25	46	23	13	93	37	15

Table 9 Global performance for cases (1–6) of Lane-Emden model.

Case	GFIT		GMAD		GRMSE		GTIC	
	Mag	SD	Mag	SD	Mag	SD	Mag	SD
1	5.29E-04	1.85E-03	3.60E-03	8.42E-03	3.66E-03	8.54E-03	5.16E-07	1.03E-06
2	1.11E-03	3.89E-03	4.24E-03	9.89E-03	4.81E-03	1.13E-02	6.89E-07	1.38E-06
3	6.06E-03	3.56E-02	5.61E-03	2.26E-02	6.39E-03	2.55E-02	7.75E-07	2.96E-06
4	5.07E-02	2.87E-01	1.66E-02	1.10E-01	1.70E-02	1.11E-01	2.09E-06	1.33E-05
5	2.98E-02	2.84E-01	5.57E-03	1.87E-02	6.43E-03	2.21E-02	9.31E-07	2.64E-06
6	6.48E-02	4.39E-01	3.24E-02	1.18E-01	3.60E-02	1.34E-01	4.51E-06	1.57E-05

Table 10 Complexity analysis for cases (1–6) of Lane-Emden model.

Case	Generation/Iteration		Time of execution		Function Counts	
	Mean	SD	Mean	SD	Mean	SD
1	170.6794	155.1256	492.01	279.9201	46055.45	19278.42
2	174.8195	162.6908	498.3	280.3729	46249.79	18818.14
3	189.8958	159.454	570.01	262.5481	50665.97	17410.45
4	188.4489	161.5488	533.53	270.1939	48694.47	18269.01
5	325.7306	1421.96	503.62	274.4711	46678.66	18511.97
6	228.1427	181.5433	628.94	223.0223	54985.35	15166.35

appeared to influence the work reported in this paper. This paper is partially supported by Ministerio de Ciencia, Innovación y Universidades grant number PGC2018-097198-B-I00 and Fundación Séneca de la Región de Murcia grant number 20783/PI/18.

References

[1] K. Diethelm, N.J. Ford, Analysis of fractional differential equations, Journal of Mathematical Analysis and Applications 265 (2) (2002) 229–248.

[2] F. Yu, Integrable coupling system of fractional soliton equation hierarchy, Phys. Lett. A 373 (41) (2009) 3730–3733.

[3] S. Momani, R.W. Ibrahim, On a fractional integral equation of periodic functions involving Weyl-Riesz operator in Banach algebras, Journal of Mathematical Analysis and Applications 339 (2) (2008) 1210–1219.

[4] R.W. Ibrahim, S. Momani, On the existence and uniqueness of solutions of a class of fractional differential equations, Journal of Mathematical Analysis and Applications 334 (1) (2007) 1–10.

[5] B. Bonilla, M. Rivero, J.J. Trujillo, On systems of linear fractional differential equations with constant coefficients, Appl. Math. Comput. 187 (1) (2007) 68–78.

[6] I. Podlubny, Fractional Differential Equations", Acade- mic Press, London, 1999.

[7] K. Diethelm, A.D. Freed, in: On the solution of nonlinear fractional-order differential equations used in the modeling of viscoplasticity, Springer, Berlin, Heidelberg, 1999, pp. 217–224.

[8] I. Podlubny, L. Dorcak, I. Kostial, December). On fractional derivatives, fractional-order dynamic systems and PI/sup/spl lambda//D/sup/spl mu//-controllers Vol. 5 (1997) 4985–4990.

[9] O.P. Agrawal, Application of fractional derivatives in thermal analysis of disk brakes, Nonlinear Dyn. 38 (1–4) (2004) 191–206.

[10] P.J. Torvik, R.L. Bagley, On the appearance of the fractional derivative in the behavior of real materials, J. Appl. Mech. 51 (2) (1984) 294–298.

[11] S. Momani, Z. Odibat, Analytical approach to linear fractional partial differential equations arising in fluid mechanics, Phys. Lett. A 355 (4–5) (2006) 271–279.

[12] R. Hilfer, Experimental evidence for fractional time evolution in glass forming materials, Chem. Phys. 284 (1–2) (2002) 399–408.

[13] N. Engheia, On the role of fractional calculus in electromagnetic theory, IEEE Antennas Propag. Mag. 39 (4) (1997) 35–46.

[14] N. Makris, M.C. Constantinou, Fractional-derivative Maxwell model for viscous dampers, J. Struct. Eng. 117 (9) (1991) 2708–2724.

[15] H. Jiang, Y. Cheng, L. Yuan, F. An, K. Jin, A fractal theory based fractional diffusion model used for the fast desorption process of methane in coal. Chaos: An Interdisciplinary, Journal of Nonlinear Science 23 (3) (2013) 033111.

[16] S. Kumar, A. Kumar, B. Samet, J.F. Gómez-Aguilar, M.S. Osman, A chaos study of tumor and effector cells in fractional tumor-immune model for cancer treatment, Chaos, Solitons Fractals 141 (2020) 110321.

[17] E. İlhan, İ.O. Kıymaz, A generalization of truncated M-fractional derivative and applications to fractional differential equations, Applied Mathematics and Nonlinear Sciences 5 (1) (2020) 171–188.

[18] J. Singh, D. Kumar, Z. Hammouch, A. Atangana, A fractional epidemiological model for computer viruses pertaining to a new fractional derivative, Appl. Math. Comput. 316 (2018) 504–515.

[19] S. Kumar, R. Kumar, M.S. Osman, B. Samet, A wavelet based numerical scheme for fractional order SEIR epidemic of measles by using Genocchi polynomials https://doi.org/10.1002/num.22577, Numerical Methods for Partial Differential Equations (2020).

[20] A. Yokuş, S. Gülbahar, Numerical solutions with linearization techniques of the fractional Harry Dym equation, Applied Mathematics and Nonlinear Sciences 4 (1) (2019) 35–42.

[21] W. Gao, P. Veeresha, D.G. Prakasha, H.M. Baskonus, G. Yel, New approach for the model describing the deathly disease in pregnant women using Mittag-Leffler function, Chaos, Solitons Fractals 134 (2020) 109696.

[22] M. Jleli, S. Kumar, R. Kumar, B. Samet, Analytical approach for time fractional wave equations in the sense of Yang-Abdel-Aty-Cattani via the homotopy perturbation transform method, Alexandria Engineering Journal 59 (5) (2020) 2859–2863.
[23] W. Gao, P. Veeresha, D.G. Prakasha, H.M. Baskonus, New numerical simulation for fractional Benney-Lin equation arising in falling film problems using two novel techniques, Numerical Methods for Partial Differential Equations 37 (1) (2020) 210–243.
[24] W. Gao, G. Yel, H.M. Baskonus, C. Cattani, Complex solitons in the conformable (2+ 1)-dimensional Ablowitz-Kaup-Newell-Segur equation, Aims Math 5 (1) (2020) 507–521.
[25] K.M. Saad, M.M. Khader, J.F. Gómez-Aguilar, D. Baleanu, Numerical solutions of the fractional Fisher's type equations with Atangana-Baleanu fractional derivative by using spectral collocation methods. Chaos: An Interdisciplinary, Journal of Nonlinear Science 29 (2) (2019) 023116.
[26] Solís-Pérez, J.E. and Gómez-Aguilar, J.F., Variable-order fractal-fractional time delay equations with power, exponential and Mittag-Leffler laws and their numerical solutions. Engineering with Computers, (10.1007/s00366-020-01065-0) pp.1-23 2020.
[27] H. Safdari, Y.E. Aghdam, J.F. Gómez-Aguilar, Shifted Chebyshev collocation of the fourth kind with convergence analysis for the space–time fractional advection-diffusion equation, Engineering with Computers 118 (2020) 1–12.
[28] C.Z. Aguilar, J.F. Gómez-Aguilar, V.M. Alvarado-Martínez, H. M. Romero-Ugalde, Fractional order neural networks for system identification, Chaos, Solitons Fractals 130 (2020) 109444.
[29] C.J. Zúñiga-Aguilar, A. Coronel-Escamilla, J.F. Gómez-Aguilar, V.M. Alvarado-Martínez, H.M. Romero-Ugalde, New numerical approximation for solving fractional delay differential equations of variable order using artificial neural networks, The European Physical Journal Plus 133 (2) (2018) 1–16.
[30] C.J. Zúñiga-Aguilar, H.M. Romero-Ugalde, J.F. Gómez-Aguilar, R.F. Escobar-Jiménez, M. Valtierra-Rodríguez, Solving fractional differential equations of variable-order involving operators with Mittag-Leffler kernel using artificial neural networks, Chaos, Solitons Fractals 103 (2017) 382–403.
[31] K.M. Saad, J.F. Gómez-Aguilar, A.A. Almadiy, A fractional numerical study on a chronic hepatitis C virus infection model with immune response, Chaos, Solitons Fractals 139 (2020) 110062.
[32] A. Coronel-Escamilla, J.F. Gomez-Aguilar, I. Stamova, F. Santamaria, Fractional order controllers increase the robustness of closed-loop deep brain stimulation systems, Chaos, Solitons Fractals 140 (2020) 110149.
[33] K.L. Wang, S.W. Yao, Y.P. Liu, L.N. Zhang, A fractal variational principle for the telegraph equation with fractal derivatives, Fractals 28 (4) (2020) 2050058.
[34] K.L. Wang, K.J. Wang, C.H. He, Physical insight of local fractional calculus and its application to fractional Kdv–Burgers–Kuramoto equation, Fractals 27 (07) (2019) 1950122.
[35] K.L. Wang, Effect of Fangzhu's nanoscale surface morphology on water collection https://doi.org/10.1002/mma.6569, Mathematical Methods in the Applied Sciences (2020).
[36] K. Wang, He's frequency formulation for fractal nonlinear oscillator arising in a microgravity space https://doi.org/10.1002/num.22584, Numerical Methods for Partial Differential Equations. (2020).
[37] S. Kumar, A. Kumar, D. Baleanu, Two analytics methods for time-fractional nonlinear coupled Boussinesq-Burger's equations arise in propagation of shallow water waves, Nonlinear Dyn. 85 (2016) 699–715.
[38] C. Burgos, J.C. Cortés, L. Villafuerte, R.J. Villanueva, Mean square calculus and random linear fractional differential equations: Theory and applications, Applied Mathematics and Nonlinear Sciences 2 (2) (2017) 317–328.
[39] D.W. Brzeziński, Review of numerical methods for NumILPT with computational accuracy assessment for fractional calculus, Applied Mathematics and Nonlinear Sciences 3 (2) (2018) 487–502.
[40] A. Atangana, J.F. Gómez-Aguilar, Numerical approximation of Riemann-Liouville definition of fractional derivative: from Riemann-Liouville to Atangana-Baleanu, Numerical Methods for Partial Differential Equations 34 (5) (2018) 1502–1523.
[41] S. Kumar, R. Kumar, C. Cattani, B. Samet, Chaotic behaviour of fractional predator-prey dynamical system, Chaos, Solitons Fractals 135 (2020) 109811.
[42] Veeresha, P., Prakasha, D.G. and Kumar, S., A fractional model for propagation of classical optical solitons by using nonsingular derivative. Mathematical Methods in the Applied Sciences. https://doi.org/10.1002/mma.6335 (2020).
[43] Safare, K.M., Betageri, V.S., Prakasha, D.G., Veeresha, P. and Kumar, S., 2020. A mathematical analysis of ongoing outbreak COVID-19 in India through nonsingular derivative. Numerical Methods for Partial Differential Equations, to appear..
[44] M. Tahir, S. Kumar, H. Rehman, M. Ramzan, A. Hasan, M.S. Osman, Exact traveling wave solutions of Chaffee-Infante equation in (2+ 1)-dimensions and dimensionless Zakharov equation, Mathematical Methods in the Applied Sciences 44 (2) (2020) 1500–1513.
[45] S. Kumar, S. Ghosh, R. Kumar, M. Jleli, A fractional model for population dynamics of two interacting species by using spectral and Hermite wavelets methods, Numerical Methods for Partial Differential Equations (2020), https://doi.org/10.1002/num.22602 (2020).
[46] A. Yıldırım, T. Öziş, Solutions of singular IVPs of Lane-Emden type by homotopy perturbation method, Phys. Lett. A 369 (1–2) (2007) 70–76.
[47] K. Parand, A. Pirkhedri, Sinc-collocation method for solving astrophysics equations, New Astron. 15 (6) (2010) 533–537.
[48] A. Yıldırım, T. Öziş, Solutions of singular IVPs of Lane-Emden type by the variational iteration method, Nonlinear Anal. Theory Methods Appl. 70 (6) (2009) 2480–2484.
[49] K. Parand, M. Dehghan, A.R. Rezaei, S.M. Ghaderi, An approximation algorithm for the solution of the nonlinear Lane-Emden type equations arising in astrophysics using Hermite functions collocation method, Comput. Phys. Commun. 181 (6) (2010) 1096–1108.
[50] E.H. Doha, W.M. Abd-Elhameed, Y.H. Youssri, Second kind Chebyshev operational matrix algorithm for solving differential equations of Lane-Emden type, New Astron. 23 (2013) 113–117.
[51] S.A. Yousefi, Legendre wavelets method for solving differential equations of Lane-Emden type, Appl. Math. Comput. 181 (2) (2006) 1417–1422.
[52] K. Parand, M. Nikarya, J.A. Rad, Solving non-linear Lane-Emden type equations using Bessel orthogonal functions collocation method, Celest. Mech. Dyn. Astron. 116 (1) (2013) 97–107.
[53] M.S. Mechee, N. Senu, Numerical study of fractional differential equations of Lane-Emden type by method of collocation, Applied Mathematics 3 (08) (2012) 851.
[54] Z. Masood et al, Design of Mexican Hat Wavelet neural networks for solving Bratu type nonlinear systems, Neurocomputing 221 (2017) 1–14.
[55] M.A.Z. Raja, S.A. Niazi, S.A. Butt, An intelligent computing technique to analyze the vibrational dynamics of rotating electrical machine, Neurocomputing 219 (2017) 280–299.
[56] J. Berg, K. Nyström, A unified deep artificial neural network approach to partial differential equations in complex geometries, Neurocomputing 317 (2018) 28–41.

[57] M. Pakdaman, A. Ahmadian, S. Effati, S. Salahshour, D. Baleanu, Solving differential equations of fractional order using an optimization technique based on training artificial neural network, Appl. Math. Comput. 293 (2017) 81–95.
[58] A. Jafarian, S.M. Nia, A.K. Golmankhaneh, D. Baleanu, On artificial neural networks approach with new cost functions, Appl. Math. Comput. 339 (2018) 546–555.
[59] B. Ghanbari, S. Kumar, R. Kumar, A study of behaviour for immune and tumor cells in immunogenetic tumour model with non-singular fractional derivative, Chaos, Solitons Fractals 133 (2020) 109619.
[60] M. Umar et al, Intelligent computing for numerical treatment of nonlinear prey–predator models, Appl. Soft Comput. 80 (2019) 506–524.
[61] I. Ahmad et al, Novel applications of intelligent computing paradigms for the analysis of nonlinear reactive transport model of the fluid in soft tissues and microvessels, Neural Comput. Appl. 31 (2019) 9041–9059.
[62] M.A.Z. Raja, F.H. Shah, M. Tariq, I. Ahmad, Design of artificial neural network models optimized with sequential quadratic programming to study the dynamics of nonlinear Troesch's problem arising in plasma physics, Neural Comput. Appl. 29 (6) (2018) 83–109.
[63] Z. Sabir et al, Neuro-heuristics for nonlinear singular Thomas-Fermi systems, Appl. Soft Comput. 65 (2018) 152–169.
[64] M.A.Z. Raja, J. Mehmood, Z. Sabir, A.K. Nasab, M.A. Manzar, Numerical solution of doubly singular nonlinear systems using neural networks-based integrated intelligent computing, Neural Comput. Appl. 31 (3) (2019) 793–812.
[65] A. Mehmood et al, Integrated intelligent computing paradigm for the dynamics of micropolar fluid flow with heat transfer in a permeable walled channel, Appl. Soft Comput. 79 (2019) 139–162.
[66] A. Mehmood et al, Intelligent computing to analyze the dynamics of magnetohydrodynamic flow over stretchable rotating disk model, Appl. Soft Comput. 67 (2018) 8–28.
[67] M.A.Z. Raja, F.H. Shah, E.S. Alaidarous, M.I. Syam, Design of bio-inspired heuristic technique integrated with interior-point algorithm to analyze the dynamics of heartbeat model, Appl. Soft Comput. 52 (2017) 605–629.
[68] W. He, Y. Chen, Z. Yin, Adaptive neural network control of an uncertain robot with full-state constraints, IEEE Trans. Cybern. 46 (3) (2016) 620–629.
[69] M.A.Z. Raja, M. Umar, Z. Sabir, J.A. Khan, D. Baleanu, A new stochastic computing paradigm for the dynamics of nonlinear singular heat conduction model of the human head, The European Physical Journal Plus 133 (9) (2018) 364.
[70] F. Pelletier, C. Masson, A. Tahan, Wind turbine power curve modelling using artificial neural network, Renewable Energy 89 (2016) 207–214.
[71] A. Zameer et al, Intelligent and robust prediction of short term wind power using genetic programming based ensemble of neural networks, Energy Convers. Manage. 134 (2017) 361–372.
[72] S. Lodhi, M.A. Manzar, M.A.Z. Raja, Fractional neural network models for nonlinear Riccati systems, Neural Comput. Appl. 31 (1) (2019) 359–378.
[73] M.A.Z. Raja, R. Samar, M.A. Manzar, S.M. Shah, Design of unsupervised fractional neural network model optimized with interior point algorithm for solving Bagley-Torvik equation, Math. Comput. Simul 132 (2017) 139–158.
[74] M. Artar, A.T. Daloğlu, Optimum weight design of steel space frames with semi-rigid connections using harmony search and genetic algorithms, Neural Comput. Appl. 29 (11) (2018) 1089–1100.
[75] C.A.C. Flórez, J.M. Rosário, D. Amaya, Control structure for a car-like robot using artificial neural networks and genetic algorithms, Neural Comput. Appl. 32 (2020) 15771–15784.
[76] J.M. Adánez, B.M. Al-Hadithi, A. Jiménez, Multidimensional membership functions in T-S fuzzy models for modelling and identification of nonlinear multivariable systems using genetic algorithms, Appl. Soft Comput. 75 (2019) 607–615.
[77] B.J. de Almeida, R.F. Neves, N. Horta, Combining Support Vector Machine with Genetic Algorithms to optimize investments in Forex markets with high leverage, Appl. Soft Comput. 64 (2018) 596–613.
[78] M. Peker, A fully customizable hardware implementation for general purpose genetic algorithms, Appl. Soft Comput. 62 (2018) 1066–1076.
[79] J.R. Fernández, J.A. López-Campos, A. Segade, J.A. Vilán, A genetic algorithm for the characterization of hyperelastic materials, Appl. Math. Comput. 329 (2018) 239–250.
[80] H. Bonakdari, Z.S. Khozani, A.H. Zaji, N. Asadpour, Evaluating the apparent shear stress in prismatic compound channels using the Genetic Algorithm based on Multi-Layer Perceptron: A comparative study, Appl. Math. Comput. 338 (2018) 400–411.
[81] D. Tian, J. Deng, G. Vinod, T.V. Santhosh, H. Tawfik, A constraint-based genetic algorithm for optimizing neural network architectures for detection of loss of coolant accidents of nuclear power plants, Neurocomputing 322 (2018) 102–119.
[82] X. Pei, Y. Zhou, N. Wang, A Gaussian process regression based on variable parameters fuzzy dominance genetic algorithm for B-TFPMM torque estimation, Neurocomputing 335 (2019) 153–169.
[83] S. Zhong, X. Xie, L. Lin, F. Wang, Genetic algorithm optimized double-reservoir echo state network for multi-regime time series prediction, Neurocomputing 238 (2017) 191–204.
[84] Raja, M.A.Z., Mehmood, A., ur Rehman, A., Khan, A. and Zameer, A., Bio-inspired computational heuristics for Sisko fluid flow and heat transfer models. Applied Soft Computing, 71 pp.622-648 (2018).
[85] M.H. Zhao, X.F. Ding, Z.H. Shi, Q.Z. Yao, Y.Q. Yuan, R.Y. Mo, An efficient active set method for optimization extreme learning machines, Neurocomputing 174 (2016) 187–193.
[86] C.P. Brás, A. Fischer, J.J. Júdice, K. Schönefeld, S. Seifert, A block active set algorithm with spectral choice line search for the symmetric eigenvalue complementarity problem, Appl. Math. Comput. 294 (2017) 36–48.
[87] I. Ahmad et al, Intelligent computing to solve fifth-order boundary value problem arising in induction motor models, Neural Comput. Appl. 29 (7) (2018) 449–466.
[88] S. Kumar, A new analytical modelling for fractional telegraph equation via Laplace transform, Appl. Math. Model. 38 (13) (2014) 3154–3163.
[89] N. Chamakuri, K. Kunisch, Primal-dual active set strategy for large scale optimization of cardiac defibrillation, Appl. Math. Comput. 292 (2017) 178–193.